Unexpected Partial Crystallization of an Amorphous Polyamide as Induced by Combined Temperature and Humidity

Amparo López-Rubio, Rafael Gavara, Jose M. Lagarón

Institute of Agrochemistry and Food Technology (IATA), CSIC, Apdo. Correos 73, E-46100 Burjassot, Spain

Received 16 December 2005; accepted 6 March 2006
DOI 10.1002/app.24430
Published online in Wiley InterScience (www.interscience.wiley.com).

ABSTRACT: In this study, it is presented for the first time, the characterization of an amorphous polyamide after having been subjected to humid thermal conditions such as those typically applied in the industrial sterilization of packaged foods. From a fundamental point of view, it was fortuitously found that the combination of heat and moisture, with and without the assistance of pressure, was capable of inducing some crystallization in the otherwise amorphous polymer. Characterization of the crystallization process was carried out by differential scanning calorimetry, Fourier transform infrared, and simultaneous time-resolved small and wide angle X-ray scattering synchrotron experiments. The crystallization of the polymer began as characterized by wide angle X-ray scattering and differential scanning calorimetry in the presence of humidity at ~90°C and extended up to 120°C under autoclave conditions, and it is thought to be the result of heated moisture being able to disrupt the intense amide groups self-association. Thus, the thermally activated molecular structure is thought to become plasticized by the combined presence of heat and water which, in turn, provoke sufficient segmental molecular mobility in the system to promote some degree of lateral order. Propertywise, the resulting consequences of this behavior are an increase in the barrier properties to oxygen and a reduction in water sorption. From an applied view point, it is suggested that this unexpected behavior could make this polymer of significant interest in retortable food packaging applications. J Appl Polym Sci 102: 1516–1523, 2006

Key words: amorphous polyamide; industrial polymers and applications; food packaging

INTRODUCTION

Because of the excellent properties of polymers as packaging materials, there is a trend in the food industry toward the replacement of classic packages manufactured with materials like glass or tinplate, with lighter, cheaper, and versatile plastic packages. These polymeric structures must, however, ensure the quality and safety of the packaged products without compromising their shelf-life.

Many food products are to be packaged with high-barrier polymeric materials because oxygen is a ubiquitous element involved in many food deterioration reactions, such as fat oxidation, vitamin loss, etc. But furthermore, several food products, like the continuously increasing demanded precooked foods (ready-to-eat products), require a retorting treatment inside the package before being commercialized (typically 121°C during 20 min in an industrial autoclave, i.e., in the presence of pressurized water vapor).[1] Thus, apart from the already mentioned high-barrier conditions, plastic packages must withstand such kind of processes without suffering undesirable changes.

Ethylene vinyl alcohol (EVOH) copolymers are a family of semicrystalline high-barrier materials commonly used in retortable packaging structures. Because of their high water sensitivity, derived from the presence of hydroxyl groups in their structure, EVOH copolymers are used as intermediate high-barrier layer in multilayer structures protected from the external relative humidity by at least two layers of a hydrophobic material such as polypropylene (PP). However, it is common knowledge that even protected between these hydrophobic materials, retorting processes have a tremendous impact on the gas barrier performance of the copolymers. Tsai and Jenkins[2] reported that the oxygen barrier of retortable packages containing an EVOH barrier layer was initially reduced by two orders of magnitude when these containers were subjected to steam or pressurized water during thermal processing and, during long-term storage (> 200 days), the barrier was partially recovered (by a factor of 10). In a more recent

Correspondence to: J. M. Lagarón (lagaron@iata.csic.es).
Contract grant sponsor: IHP (European Commission); contract grant number: HPRI-CT-1999-00,040/2001-00,140.
Contract grant sponsor: FPI (Spanish Ministry of Education and Science); contract grant number: AGL2003-07,326-C02-01.
Contract grant sponsor: CYCYT; contract grant number: MAT2003-08,480-C03.

work,[3] it was demonstrated that this huge increase in permeability was caused not only by the plasticization of the EVOH structure, as it had been previously reported,[2,4] but also by a deterioration of the copolymer crystallinity that takes place in multilayer structures during the retorting process.[5] Real-time experiments during *in situ* retorting of EVOH monolayers showed that the material melts around 100°C, which implies that the polymer melts 83°C earlier than expected in the presence of heated water vapor.[3] This behavior clearly proves the strong moisture sensitivity of the material even in multilayer structures.

As a consequence of the detrimental effects of common retorting processes over the structure and permeability of the EVOH copolymers, alternative high-barrier materials are being studied as potential substitutes in retortable food packaging structures. Aliphatic polyketones and amorphous PA are high and medium-high barrier materials with potential in retortable applications. A very recent study has already proven that the aliphatic polyketones are adequate materials to withstand packaged food retorting conditions, as the deterioration in oxygen barrier suffered by these polymers even in monolayer structures is very small compared with the deterioration suffered by EVOH based multilayer structures.[6] Amorphous polyamides (aPAs), on the other hand, offer favorable properties such as dimensional stability, good dielectric and barrier properties, and low mold shrinkage,[7] and, furthermore, exhibit an antiplasticization behavior at high relative humidity conditions. Thus, it is known that the oxygen barrier performance of this material increases at high relative humidity conditions in contrast with the behavior of most polar polymers, including most polyamides, aliphatic polyketones, and EVOH.[8] It is, therefore, of significant relevance to study the effect of common humid thermal processes for this polymer regarding its potential inclusion in retortable food packaging structures.

In this overall context, this original study reports on the structural and oxygen barrier alterations suffered by a commercial aPA material during temperature, humidity, and combined temperature and humidity (autoclaved or retorting) treatments by means of differential scanning calorimetry (DSC), Fourier transform infrared (FTIR), oxygen transmission rate, and simultaneous wide and small angle X-ray scattering (WAXS and SAXS) experiments via synchrotron radiation.

MATERIALS AND METHODS

An aPA experimental grade (SELAR UX-2034) from Dupont (U.S.) polymerized by the condensation of hexamethylene diamine and a mixture of 70 : 30 isophthalic and terephthalic acids was used in a film extruded form. Alternatively, multilayer structures were obtained by vacuum sealing the aPA between PP layers with a typical nominal thickness of the barrier layer around 45 μm. As no tie layers were used, the intermediate aPA barrier layer studied here could be easily peeled off after the treatment for testing. Unless otherwise stated, all the samples were kept in a dessicator for a week before testing.

Thermal treatments

The materials were thermally treated under dry and humid conditions in a conventional oven (annealing) and in an autoclave (retorting), respectively. The standard treatment given to the samples, both in the oven and in the autoclave, was 120°C during 20 min. The material was also heated in boiling water for 20 min to discriminate the water vapor pressure effect from the combined temperature and humidity effect.

Oxygen transmission rate

O_2TR values were obtained from an OXTRAN 2/20 (Mocon, US). The samples were placed in a 5 cm^2 test cell and the measurements were made using a gas flux of 10 mL/min, ambient temperature (around 24°C), and a relative humidity of 0%. The O_2TR values were corrected with the thickness of the films and with the pressure gradient of the experiment, i.e., 1 atm. The oxygen transmission rate of the untreated aPA was measured in dry until equilibrium permeability was reached. A similar sample was vacuum sealed between two PP layers and retorted in the autoclave during 20 min at 120°C. After the retorting treatment, the multilayer structure was delaminated and the aPA intermediate layer was immediately placed in the OXTRAN cell and its oxygen transmission rate was measured as a function of time.

Attenuated total reflection/FTIR spectroscopy

Attenuated total reflection (ATR) infrared (IR) experiments were carried out coupling the Golden Gate ATR accessory (Specac, Orpiugtou, UK) to a FTIR Tensor 37 (Bruker, Rheiustetlen, Germany) spectrometer with a resolution of 4 cm^{-1}. Typical acquisition times were about 10 s.

Differential scanning calorimetry

DSC experiments were carried out in a Perkin–Elmer DSC-7 calorimeter. The heating and cooling rate for the runs was 10°C/min, being the typical sample weight around 4 mg. Calibration was performed using an indium sample. All tests were carried out, at least, in duplicate to check for repeatability. The temperature range of the assays was from 50 to 250°C. From the thermograms, the glass transition temperature (T_g) was

determined from the temperature of half the change of the specific heat. Apart from the aluminum pans used to perform the previous experiments, pressure proof steel pans were also used to simulate a retorting process. The steel pans are designed to resist the vapor pressure built up exerted during temperature experiments with liquids or solids and, therefore, they can serve as calorimetric autoclaves to monitor *in situ* the enthalpic changes taking place during the retorting experiment. A sample of aPA was placed inside the pan with 10 μL of water where it was heated from 50 to 120°C at 10°C/min and then it was held at 120°C during 20 min. A steel reference pan with indium was used for calibrating the equipment, and another one as a reference pan containing the exact amount of water present in the sample pan to eliminate the water signal from the DSC thermograms.

X-Ray diffraction

Simultaneous WAXS and SAXS experiments were carried out at the synchrotron radiation source in the polymer beam A2 at Hasylab (DESY) in Hamburg (Germany). Scattering patterns were recorded using a one-dimensional detector and an incident radiation wavelength, λ, of 0.15 nm. WAXS and SAXS data were corrected for detector response and beam intensity and calibrated against PET and rat tail standards. Temperature scans were also carried out at 5°C/min on dry (sandwiched between aluminum foil) and in water saturation simulating an industrial retorting process. Water saturation conditions during the temperature experiment were ensured by sealing a water-saturated aPA specimen in excess of water between aluminum windows and O-ring rubber seals inside screwed rectangular cell compartments designed for measuring liquids as a function of temperature specifically designed for the experimental setup.[3] Experiment success was checked by observation of constant background intensity over the experiment and presence of moisture in the cell after termination of the thermal experiments, which indicated that moisture did not leak off the cell during the temperature run.

Sorption measurements

Water uptake was analyzed by immersing the previously dried (vacuum oven overnight at 70°C) untreated and retorted aPA directly into the solvent. Weight gain measurements were carried out at room temperature in an analytical balance model Mettler AE240. Before each measurement, the polymer surface was thoroughly wiped off with a tissue to eliminate excess solvent. The experiments were carried out in duplicate to check for reproducibility, and average values were fitted to the appropriate solution of the second law of Fick to determine diffusion coefficients.

RESULTS AND DISCUSSION

Structural characterization

After humid thermal autoclaving of an aPA specimen, it was observed that the originally transparent film became more rigid and whitish to some extent. As a result, the structural and/or morphological characteristics of the material were thought to change during the applied process. Figure 1 shows the DSC curves obtained during a typical DSC experiment (heating–cooling–heating runs) of untreated, heated in the oven, heated in boiling water, and retorted aPA specimens.

The second heating scan shows that in all cases the T_g of the untreated aPA is around 126°C. In all experiments, but in the annealed specimen, the evaporation of sorbed moisture impeded the observation of the T_g event in the first heating scan. It is assumed that as the sorption of moisture is known to decrease the T_g of the polymer, this is not observed by the presence of the dominant sorbed moisture endothermic signal covering the range from 50°C up to about 120°C.[8,9]

Surprisingly, the retorted sample displays three endothermic features, which suggests that during the combined treatment with temperature and pressurized water vapor, some degree of crystallization develops in the polymer. In the case of the high-barrier EVOH copolymer, the vapor pressure generated inside the autoclave during the autoclaving cycle was found to lead to a total disruption of the EVOH crystals. Thus, although this study was originally intended to ascertain the effects of retorting over the structure of the aPA polymers, the unexpected presence of crystallization made necessary to study what other potential effects could cause conditions such as temperature, presence of humidity, or the pressurized water vapor in the structure of the polymer. For this purpose, further analysis was

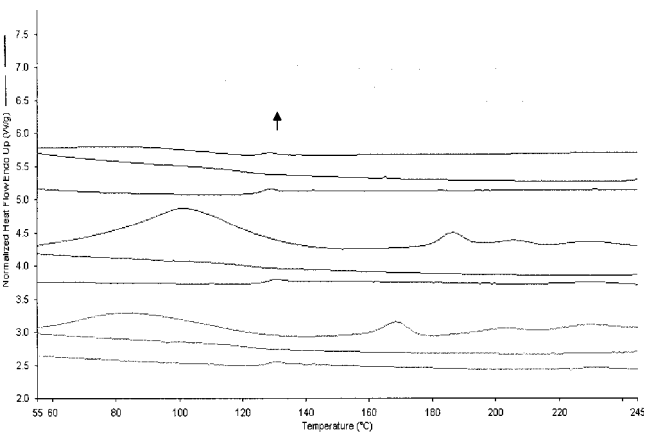

Figure 1 DSC thermograms of (from top to down): Untreated aPA, aPA heated in the oven at 120°C during 20 min, aPA retorted, and aPA heated in boiling water for 20 min. The three runs of each experiment are shown in the picture, top one being the first heating run, the middle one the cooling run, and the bottom one the second heating run.

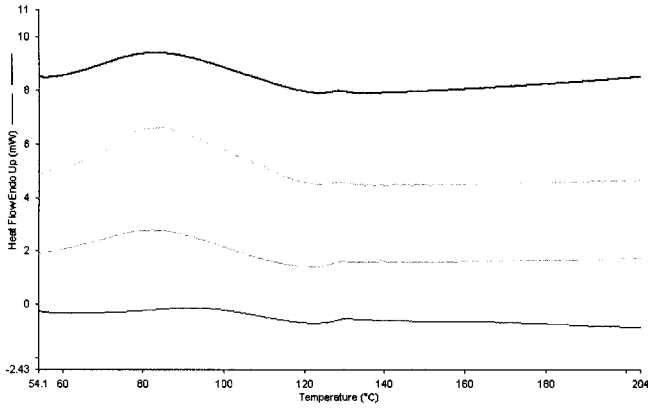

Figure 2 First heating DSC scans of aPA at different relative humidities. From top to bottom: 100, 75, 23, and 0% RH.

carried out in samples that had undergone different conditionings. From Figure 1 it can be observed that the annealing process in the oven does only conduct to the elimination of strongly bound water, and, therefore, that aside temperature, water is still needed to achieve lateral molecular order. The effect of vapor pressure on the development of crystallinity was checked by heating an specimen of aPA in boiling water, and if compared with the autoclaved polyamide, the sample also displays three endothermic peaks in the DSC but displaced toward lower temperatures (±15°C lower), pointing out that smaller or more defective crystals are formed when no vapor pressure is exerted. The enthalpy of fusion of the retorted aPA is also higher. i.e., ΔH_m[retorted] = 36 J/g and ΔH_m[heated in boiling water] = 33 J/g, indicating that a higher degree of crystallization takes place in the specimen in the autoclaved sample. Another curious observation is that in the first heating run of most samples a small endothermic transition is seen around 125°C, which from observation of the third heating scan appears as a molecular relaxation associated to the T_g event in the polymer. However, it is also well reported that the T_g of the polymer decreases in the presence of water up to a value of 54°C in a water equilibrated sample. Thus, to check for the effect that the relative humidity has on the first DSC thermogram, the material was equilibrated at different relative humidities and scanned by DSC. Figure 2 shows the first heating run of specimens equilibrated at different relative humidities. From this figure, it is seen that the above endothermic feature is located at approximately the same temperature across humidity, therefore ruling out the possibility of being associated with a T_g event in the polymer. The origin of this signal is unknown but it could be associated with a molecular relaxation process not being affected by moisture or could be related to a strongly bonded moisture signal.

What appears obvious from the DSC experiments is that the crystallinity is heterogeneous in size or perfection because of the multiple melting endotherms observed, and that this does only occur in the presence of humidity, because in the crystallization and subsequent second melting step under nitrogen atmosphere this is no longer detected (see Fig. 1). From previous work, it was found that the polymer is not able to disrupt the originally present hydrogen bonding network between amide groups as a result of moisture sorption.[9] From the present results, however, it seems apparent that this material requires of heated moisture to weaken the strong intermolecular and intramolecular bonding network established between the amide groups needed to rearrange certain chain segments in a way to achieve some lateral order.

The molecular structure of the autoclaved aPA was also analyzed by FTIR spectroscopy. The FTIR spectra of dry aPA and retorted aPA specimens are presented in Figure 3. The assignment of the major IR bands of interest is summarized in Table I.

Figure 3(a) shows the CH/CH_2 and NH stretching range normalized to the intensity of the CH_2 symmetric stretch band at 2850 cm^{-1} for comparison purposes. The intensity of the latter band has been found to be

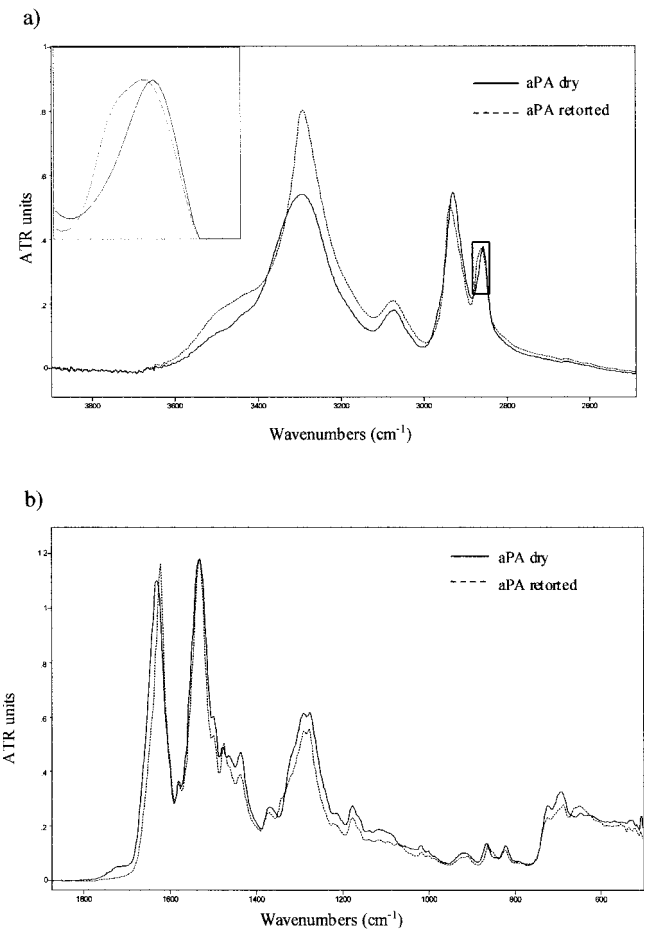

Figure 3 ATR-FTIR spectra of dry (continuous) and retorted (dashed) aPA specimens. (a) N—H and C—H stretching regions in the range 2600–3800 cm^{-1}; (b) amide I, II, III, and V regions in the range 600–1800 cm^{-1}.

TABLE I
aPA FTIR Bands of Interest and Their Most Likely Assignments

Wavenumbers (cm^{-1})	Band assignment
3444	''Free'' N—H stretch
3310	Hydrogen-bonded N—H stretch
3070	Aromatic C—H stretch
2930	Asymmetric CH_2 stretch
2850	Symmetric CH_2 stretch
1630	Amide I mode
1535	Amide II mode
~ 1290	Amide III mode
700	Amide V mode

unaffected by water sorption and has been used before as internal standard for this polymer.[8] However, because of the partial crystallization of the autoclaved specimen, this band is no longer adequate as internal standard in this study as it is usually sensitive to conformational changes. Irrespective of this, it is clear from observation of this figure that several absorption bands have changed shape, position, and/or relative intensity. It is known that when a polymer sample crystallizes either new absorption bands and/or narrowing of the spectral features is often observed because of an increase in conformational regularity and other resulting effects like factor group splitting, etc.[10] From observation of the spectrum, new bands and narrowing of some spectral features does take place (see Fig. 3).

The main difference between the two spectra is observed in the *N*—H stretching region, which covers a range of about 3100–3500 cm^{-1}. The *N*—H stretching vibration is not a conformationally sensitive mode, but it is strongly sensitive to changes in hydrogen bonding. In a simplistic interpretation, the broad band envelope can be considered to be composed of two bands, namely, a dominant band centered at 3310 cm^{-1} attributed to a distribution of hydrogen-bonded *N*—H groups, and a higher frequency small shoulder band centered at 3444 cm^{-1} attributed to ''free'' *N*—H groups. In the presence of humidity, other water bands are observed in this vibrational range. In a previous study dealing with the FTIR spectrum of this sample,[8,11] up to five different bands were found to constitute the complex band profile underlying this range.

The broadness of the hydrogen-bonded *N*—H band reflects, in large part, the distribution of hydrogen-bonded *N*—H groups of varying strengths dictated by distance and geometry. Given the ''spaghetti like'' nature of random chain molecules, it is expected that there will be a distribution of distances and geometries of these hydrogen bonds formed between complementary *N*—H and C=O moieties.[11] However, after retorting, the highly absorbent *N*—H stretching mode at 3310 cm^{-1} gets narrower; this indicates a more regular distribution and geometry of the *N*—H group vibrations. Moreover, the mentioned band appears to increase relative intensity and has slightly shifted toward lower wavenumbers. This tendency is opposite to that observed in the work of Skrovanek et al.,[11] which described the effect of temperature in the FTIR spectrum of an aPA. In the latter work, the authors found that with increasing temperature, the IR active NH stretch band was found to shift toward higher wavenumbers and to decrease in intensity. The band shift reflects a decrease in the average NH bond length because of temperature-induced weakening of the polymer self-association, while the reduction in area of the hydrogen bonded *N*—H stretching mode with increasing temperature was mainly attributed to a decrease in the absorption coefficient. The latter result can be explained by the strong dependence found between the absorptivity coefficient and the hydrogen bond strength. Therefore, the apparently higher intensity displayed by this band in the retorted specimen would indicate both a narrowing effect of the band and a higher hydrogen bond strength which, in turn, will result in a more regular conformational state of the aPA polymer chains as in crystals.

Although both aPA samples (untreated and retorted) were dried in a desiccator before taking the IR spectra, the water band displayed in both spectra at approximately 3491 cm^{-1} overlaps with the ''free'' *N*—H groups, making difficult its quantification.

In contrast with the results observed in the case of water sorption,[8] after autoclaving, the aromatic CH stretching band at 3075 cm^{-1} is seen to shift to lower wavenumbers, and the band corresponding to the CH symmetric stretching seems to split into two different components probably because of correlation field splitting or factor group splitting effects [see inset in Fig. 3(a)]. The latter observation strongly points again to the presence of crystalline order in the polymer.

The amide I and II modes are conformationally sensitive and, therefore, frequency shifts of these bands can also be related to changes in the conformation of the polymer chains. However, unlike the essentially isolated *N*—H stretching vibration, the amide I and II modes are more complex vibrations containing contributions from different functional groups (bond vibrations) and, as a result, the changes observed are difficult to interpret.

The amide I mode at 1630 cm^{-1}, which is considered to be composed of contributions from mainly the C=O stretching and also from the C—N stretching and the C—C—N deformation vibrations, shifts toward lower wavenumbers and gets narrower after the retorting of the material. The amide II mode is a mixed mode containing contributions from the *N*—H in-plane bending, the C—N stretching, and the C—C stretching vibrations. This band at 1535 cm^{-1} also gets narrower and shifts toward lower wavenumbers after autoclaving. In general, it can be stated that narrower bands are related with more homogeneous bonds features, and therefore,

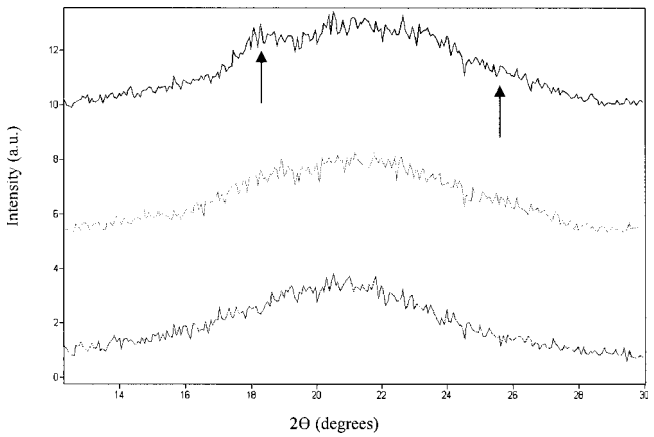

Figure 4 From top to bottom: WAXS diffraction patterns of retorted, heated in boiling water, and untreated amorphous polyamide.

with more ordered polymer structures. The displacement toward lower wavenumbers of both amide I and II modes are related with an increase in bond length. These results are thus consistent with the shift observed for the hydrogen bonded NH stretching band. The displacement toward lower wavenumbers of both, the hydrogen-bonded NH stretching band and the amide I band, are related with an increase in the bond length, and can be explained by the enhanced hydrogen bonding interactions established in the crystals and, therefore, with the presence of crystallinity.

Several changes in band shape, position, and intensity are also observed in the amide III and V modes, which indicate the substantial changes that take place in the aPA structure as a consequence of retorting. However, these modes are highly mixed and will not be discussed further in this study.

The presence of crystallinity in the retorted aPA was again confirmed by means of simultaneous SAXS and WAXS experiments in the polymer films. Figure 4 shows the WAXS patterns of an untreated, heated in boiling water and retorted aPA specimen. From this figure, it can be seen that two crystalline peaks arise in the retorted sample, namely, a more intense one at $2\theta \sim 18^\circ$ and a weak band at $2\theta \sim 26^\circ$ (see arrows). In agreement with DSC results, X-ray scattering studies also revealed the presence of crystals in the specimen heated in boiling water. Also in agreement with the DSC results, the crystallinity diffraction peaks are less clearly defined for the latter sample and are, in general, poorly defined, suggesting heterogeneity in crystal size and perfection. By curve-fitting determination of the area of the crystalline peaks under the amorphous halo of the WAXS pattern, it was found that the crystallinity of the retorted polymer film is around 5%.

The presence of periodicity at the mesoscale in the retorted aPA was further confirmed by a very weak shoulder that appears in the SAXS pattern of the retorted sample (see Fig. 5). From this plot, the maximum of the SAXS peak was determined to yield an average long period value ($L = L_c + L_a$) of 94 nm. By multiplying the repeat distance (L) by the determined crystallinity fraction, an average crystal thickness value (L_c) of approximately 4.7 nm can be derived for the retorted specimen. This indeed suggests a very ill-defined crystalline morphology for the sample.

To determine how the crystallinity develops in the sample, *in situ* time-resolved simultaneous WAXS and SAXS synchrotron experiments were carried out both on dry aPA and on the sample specimen encapsulated in the presence of water. The evolution of the WAXS patterns of the untreated (heated up to 250°C) and retorted aPA (during a typical *in situ* retorting experiment) are displayed in Figure 6. Despite the relatively high noise signal born out of the fact that the film is a poor scatterer sample, it is observed that in contrast with the amorphous halo seen along the heating of the untreated specimen, a crystalline peak at $2\theta \sim 18^\circ$ develops in the autoclaved sample and becomes clearly detectable at around 110°C. The latter peaks develop further and stay in the sample along the whole retorting experiment in agreement with the fact that after retorting the sample remains crystalline as determined by DSC.

Further *in situ* retorting experiments were also performed by DSC using sealed steel pans as retorting miniautoclaves. Figure 7(a) shows that during the initial heating step, an exothermic peak develops at ~90°C and extends up to about 120°C, with maximum at ~105°C and with a crystallization enthalpy of 28 J/g. During the 20 min isothermal step [Fig. 7(b)], no further crystallization appears to take place in the sample and this indicates that the crystallization process extends in water mostly along the heating ramp and that the crystallization endset is around 115°C. The relative broadness of the crystallization peak may explain the broad DSC multiple melting enthotherm explained in terms of a heterogeneous population of crystal size and/or perfection.

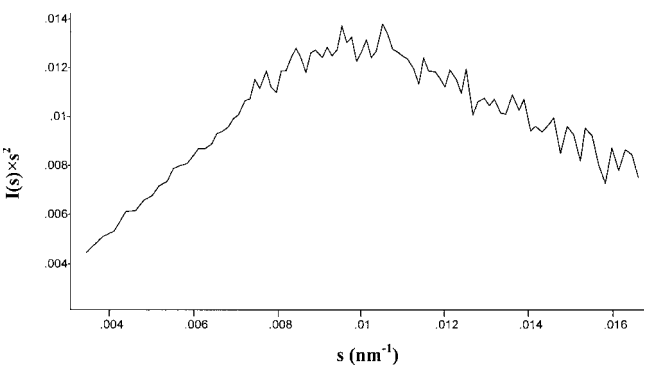

Figure 5 Lorentz-corrected SAXS pattern of retorted aPA.

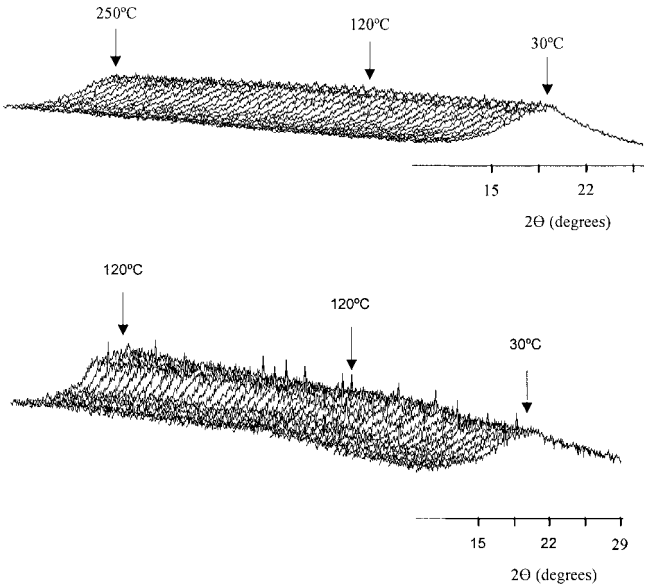

Figure 6 WAXS diffraction patterns of an amorphous polyamide during an *in situ* heating experiment up to 250°C of a dry specimen (top figure) and during an *in situ* retorting experiment in the presence of water (bottom figure).

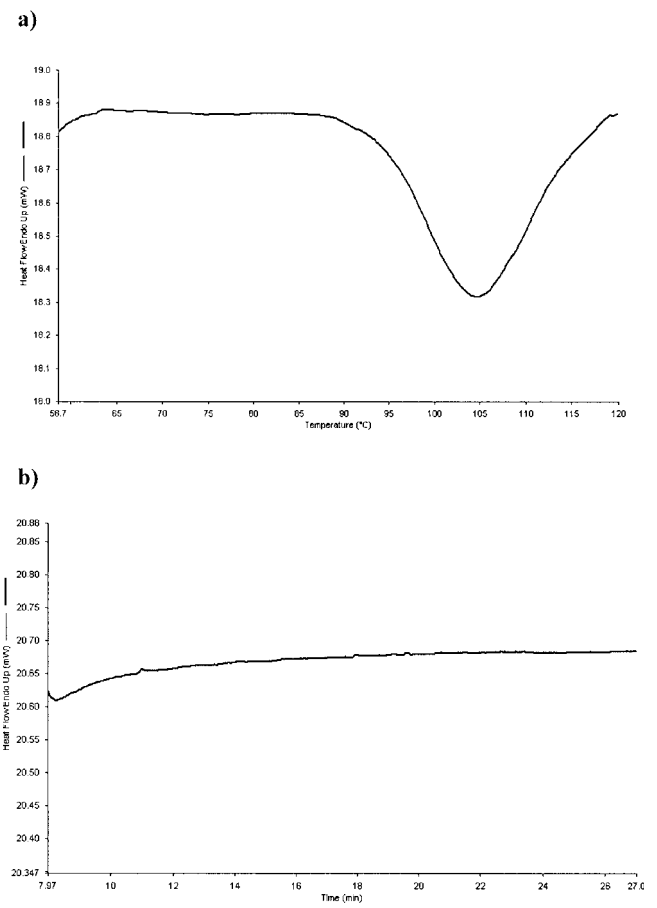

Figure 7 DSC curves of an amorphous polyamide during an *in situ* retorting experiment. (a) Heating-curve showing the formation of crystals. (b) Holding-curve at 120°C during 20 min.

Transport properties

As crystallinity defines many properties, and this material is being currently studied, in among other uses, food packaging applications, it was considered that a very relevant property for the application would be the barrier behavior for its strong implications in food quality and safety issues.

Because the material becomes rather brittle when is retorted as a monolayer and that makes difficult to clamp the film to the oxygen permeability kit without sample failure, the material was retorted sandwitched between water barrier PP layers, which is the usual multilayer configuration in retortable food packaging applications. Thus, the polyamide film was vacuum sandwiched between two layers of PP before retorting, after that the PP was delaminated and the barrier layer released for barrier testing. The sample retorted between PP also underwent crystallization as determined by DSC but to a lesser extent (the melting enthalpy of the retorted monolayer yielded 36 J/g and that of the sample autoclaved between PP layers yielded 20 J/g). The reason for this behavior is that even when the PP offers sufficient barrier to water at ambient conditions, it is well reported to allow the passage of some moisture under the high temperature conditions of the retorting process to have an impact on the barrier layer.[3]

Figure 8 shows the O_2TR curves corrected for the thickness of the aPA films and their corresponding fit to the appropriate permeability equation.[13] From Figure 8, it can be observed that not only the permeability coefficient reached a clearly lower value for the retorted specimen, but also that the average diffusion coefficient was found to be slightly lower for the crystallyzed aPA ($D_{\text{untreated aPA}} = 8.24\ 10^{-14}$ m^2/s; $D_{\text{retorted aPA}} = 7.85\ 10^{-14}$ m^2/s). As crystals are impermeable elements, these elements generally lead to diminished sol-

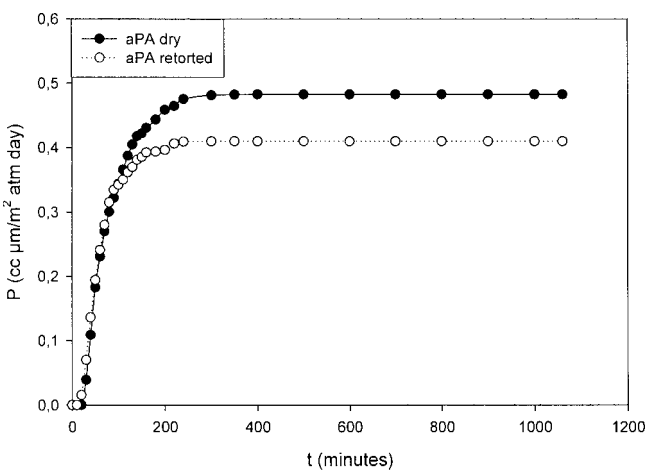

Figure 8 Oxygen permeability of untreated and retorted aPA and corresponding fits to the appropriate permeation equation.

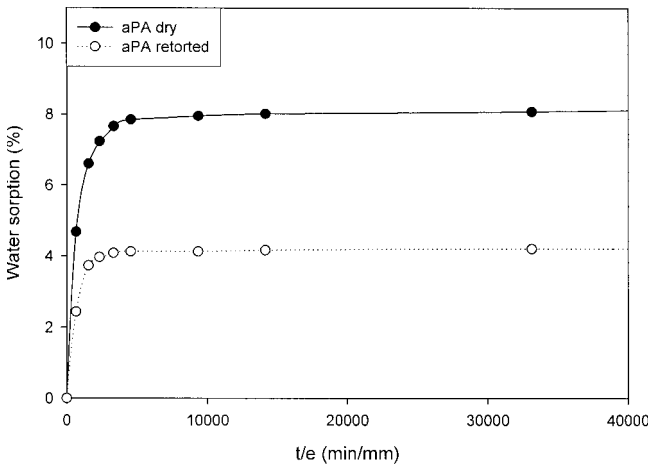

Figure 9 Water sorption of aPA dry (closed symbols) and aPA retorted (open symbols), and corresponding fits to the appropriate Fick sorption model.

ubility and diffusivity coefficients, the latter effect due to a more tortuous path for the permeant to travel across the thickness. In the equilibrium, the oxygen permeability values determined were 0.48 ± 0.008 and 0.41 ± 0.009 (cc μm)/(m^2 day atm) for the untreated and retorted aPA specimens, respectively. As a result, after retorting, there is a reduction of around 15% of the original O_2 permeability value, which, in turn, results in a better barrier performance for the retorted specimen.

Figure 9 shows the water sorption curves obtained for the untreated and retorted aPA samples and the corresponding fits to the appropriate solution to the Fick second law for a plane sheet.[14] As expected, the sorption of this solvent was lower and with slightly lower kinetics in the latter sample. The average diffusion coefficient was found to be of 8.45 10^{-14} m^2/s for the untreated sample and of 7.76 10^{-14} m^2/s for the autoclaved sample While the uptake of sorbed water is 8% (W/W_{dry}) for untreated aPA (in accordance with previous works[12]), the retorted specimen only sorbed 4%. The reason why the barrier difference is larger in water than in oxygen is probably associated to the fact that the sample tested for oxygen was autoclaved between PP protected layers, i.e., it is less crystalline, and for water sorption it was directly exposed as a monolayer.

The work was performed at the synchrotron radiation facility in Hamburg (HASYLAB, DESY, Germany). The authors thank Dr. S. Funari and Mr. M. Dommach (A2 station) for experimental support.

References

1. Ramesh, M. N. In: Handbook of Food Preservation; Rahman, S. M., Ed.; Marcel Dekker: New York, 1999; p 95.
2. Tsai, B. C.; Jenkins, B. J. J Plast Film Sheeting 1988, 4, 63.
3. López-Rubio, A.; Lagarón, J. M.; Giménez, E.; Cava, D.; Hernandez-Muñoz, P.; Yamamoto, T.; Gavara, R. Macromolecules 2003, 36, 9467.
4. Zhang, Z.; Britt, I. J.; Tung M. A. J Polym Sci Part B: Polym Phys 1999, 37, 691.
5. López-Rubio, A.; Hernandez-Muñoz, P.; Giménez, E.; Yamamoto, T.; Gavara, R.; Lagarón, J. M. J Appl Polym Sci 2005, 96, 2192.
6. López-Rubio, A.; Giménez, E.; Gavara, R.; Lagarón, J. M. J Appl Polym Sci 2006, 101, 3348.
7. Granado, A.; Eguiazábal, J. I.; Nazábal, J. Macromol Mater Eng 2004, 289, 281.
8. Lagarón, J. M.; Giménez, E.; Catalá, R.; Gavara, R. Macromol Chem Phys 2003, 204, 704.
9. Hernández, R. J.; Giacin, J. R.; Grulke, E. A. J Membr Sci 1992, 65, 187.
10. Mallapragada, S. K.; Narasimhan, B. In: Encyclopedia of Analytical Chemistry; Meyers, R. A., Ed.; Wiley: New York, 2000.
11. Skrovanek, D. J.; Howe, S. E.; Painter, P.C.; Coleman, M. M. Macromolecules 1985, 18, 1676.
12. Lagarón, J. M.; Giménez, E.; Gavara, R.; Saura, J. J. Polymer 2001, 42, 9531.
13. Liu, R. Y. F.; Schiraldi D. A.; Hiltner, A.; Baer, E. J Polym Sci Part B: Polym Phys 2002, 40, 862.
14. Crank J. The Mathematics of Diffusion, 2nd ed.; Oxford Science Publications: Oxford, UK, 1975.